

TECHNION-PH-96-21

DESY-97-051

Calculations of penguin diagrams in B decaysCaidian Lu^{a1} and Da-Xin Zhang^b^a II Institut für Theoretische Physik, Universität Hamburg, D-22761 Hamburg, Germany^b Physics Department, Technion-Israel Institute of Technology, Haifa 32000, Israel

Abstract

We analyze the effects of the space-like penguin diagrams in two body B decays $B \rightarrow K K^0$ and $B \rightarrow \bar{K} K^0$. Special attention is paid to the operator Q_6 , whose contribution is large in the BSW model, but vanishes in the PQCD method in the approximation of neglecting the masses in the final states.Suppressions of the space-like penguin diagrams are found in the PQCD method, which implies that the contributions of the space-like penguins are small compared to those of the time-like penguins.

PACS number(s): 13.25Hw, 12.15Mm, 14.40Nd, 12.38Bx

Keywords: Space-like penguin, time-like penguin, perturbative QCD

¹Alexander von Humboldt fellow.

Penguin diagrams in exclusive B decays have been of great interests in the study of CP violations[1]. Up to now, most of the quantitative investigations concentrate on the so-called time-like penguin diagrams, except in [2, 3] where, using the BSW model[4], the space-like penguin diagrams are found to be important.

An important feature of the BSW model in nonleptonic decays is the use of the factorization hypothesis[4]. Under this hypothesis, one decomposes the decay amplitude into the product of two hadronic matrix elements which are related to the leptonic or semileptonic processes. While this hypothesis works for the tree level processes if some phenomenological parameters are introduced to fit the experimental data [4, 5], there exists no firm foundation to use it in processes involving penguin diagrams. Because the penguin operators have different Lorentz structures from the tree level $(V-A)(V-A)$ ones, it is necessary to use the equations of motion for the free quarks to relate the hadronic matrix elements of these two kinds of operators[6]. However, this procedure is not proved since these equations must be used for the quarks inside hadrons. Consequently, for a special operator Q_6 [7], the decay amplitudes of the space-like penguins always involve the factor $M_B = (m_q - m_{q^0})$, where q and q^0 are light quarks[6, 2, 3]. This is a huge factor and more seriously, it might produce the singularity at $m_q = m_{q^0}$ which cannot be cured by the BSW model itself.

In this work we use the perturbative QCD (PQCD) method [8, 9] to re-analyze the penguin dominated processes $B \rightarrow K K^0$ and $B \rightarrow \bar{K} K^0$. The calculations of the decay amplitudes between the involved hadrons are replaced by those of the scattering amplitudes between the quarks, and the non-perturbative aspects of QCD are attributed to the wave functions which are taken as external inputs. Since there exists no reliable way to determine these wave functions up to now, some approximate forms (like those to be used below) were chosen in the literature as practical ways of performing phenomenological analysis. Hence the results are model dependent, like those from the BSW model[4].

Following [9], in the PQCD method there is no need of using the factorization hypothesis

or the equation of motion in the nonleptonic processes. We calculate the decay amplitudes for the penguin diagrams, and compare the contributions from the space-like and time-like penguins. We find that within PQCD there is no singularity which exists in the BSW model, and the space-like penguins are generally suppressed compared to the time-like ones.

2

We take the pure penguin processes as the examples in the following. To start, we use the effective Hamiltonian for the charmless nonleptonic B decays as [7]

$$H_{\text{eff}} = \frac{G_F}{\sqrt{2}} \sum_{i=1}^6 V_{CKM} C_i(m_b) Q_i; \quad (1)$$

where V_{CKM} denotes the CKM factors, and the operators are

$$\begin{aligned} Q_1^u &= (\bar{q}u)_{V-A} (\bar{u}b)_{V-A}; & Q_2^u &= (\bar{q}u)_{V-A} (\bar{u}b)_{V-A}; \\ Q_3 &= (\bar{q}b)_{V-A} \sum_X (\bar{q}^0 q^0)_{V-A}; & Q_4 &= (\bar{q}b)_{V-A} \sum_X (\bar{q}^0 q^0)_{V-A}; \\ Q_5 &= (\bar{q}b)_{V-A} \sum_{q^0} (\bar{q}^0 q^0)_{V+A}; & Q_6 &= (\bar{q}b)_{V-A} \sum_{q^0} (\bar{q}^0 q^0)_{V+A} \end{aligned} \quad (2)$$

for $q = d, s$ and $q^0 = u, d, s$. The operators Q_3 to Q_6 come from the penguin diagrams.

Performing the Fierz transformations, we get

$$\begin{aligned} Q_1^u &= (\bar{u}u)_{V-A} (\bar{q}b)_{V-A}; & Q_2^u &= (\bar{q}u)_{V-A} (\bar{u}b)_{V-A}; \\ Q_3 &= \sum_X (\bar{q}b)_{V-A} (\bar{q}^0 q^0)_{V-A}; & Q_4 &= \sum_X (\bar{q}b)_{V-A} (\bar{q}^0 q^0)_{V-A}; \\ Q_5 &= \sum_{q^0} (\bar{q}b)_{V-A} (\bar{q}^0 q^0)_{V+A}; & Q_6 &= \frac{1}{2} \sum_{q^0} (\bar{q}b)_{S-P} (\bar{q}^0 q^0)_{S+P}; \end{aligned} \quad (3)$$

The Wilson coefficients of (1) are [7]

$$\begin{aligned} C_1(m_b) &= 0.184; & C_2(m_b) &= 1.078; \\ C_3(m_b) &= 0.013; & C_4(m_b) &= 0.035; \\ C_5(m_b) &= 0.009; & C_6(m_b) &= 0.041; \end{aligned} \quad (4)$$

Then the amplitudes for the 2-body nonleptonic B decays are

$$\langle YZ | H_{\text{eff}} | B \rangle = \frac{G_F}{\sqrt{2}} \sum_{i=1}^6 V_{CKM} C_i(m_b) \langle YZ | Q_i | B \rangle; \quad (5)$$

In processes with penguin contributions, the amplitudes of (5) receive contributions from both time-like and space-like penguin diagrams, which are depicted in Figure 1 (a) and 1 (b).

3

Working in the BSW model, the treatments of the space-like penguin contributions of the operator Q_6 need to be discussed in some details. These treatments can be described as the following. We use the basis in (3). First, the factorization hypothesis is made to get

$$\langle Y(q_V^0 q_V^0) Z(q_V q_V^0) \mathcal{D}_6 \mathcal{B}(bq^0) \rangle = \sqrt{2} \langle Y(q_V^0 q_V^0) Z(q_V q_V^0) j(qq^0)_{S+P} \mathcal{D} \rangle \langle 0 j(qb)_{S+P} \mathcal{B}(bq^0) \rangle : \quad (6)$$

Second, use of the equations of motion [2, 3, 6]

$$qq^0 = \frac{i\partial_\mu (q_\mu - q_\mu^0)}{m_q - m_{q^0}}; \quad q^0_5 b = \frac{i\partial_\mu (q_\mu^0 - q_\mu b)}{m_b + m_{q^0}} \quad (7)$$

is needed to relate the two hadronic matrix elements on the right-handed-side of (6) to those with the usual ones with $V-A$ currents. Third, the quark currents on the right-handed-sides of (7) are approximated by their hadronic counterparts as [4]

$$qb = (qb)_H; \quad (8)$$

where the sublabels denote the hadronization. And fourth, partial differential operations on the hadronic matrix elements are used giving the final result

$$\begin{aligned} \langle Y(q_V^0 q_V^0) Z(q_V q_V^0) \mathcal{D}_6 \mathcal{B}(bq^0) \rangle &= \frac{2m_B^2}{(m_q - m_{q^0})(m_b + m_{q^0})} \\ &\langle Y(q_V^0 q_V^0) Z(q_V q_V^0) j(qq^0)_V \mathcal{D} \rangle \langle 0 j(qb)_A \mathcal{B}(bq^0) \rangle : \end{aligned} \quad (9)$$

There exist another ambiguity in the procedure described above besides the usefulness of the factorization hypothesis. In using the equations of motion in (7) we have worked at the quark level, thus the quark masses appearing in (7) seem to be the current ones. However, it

is also allowed to reverse the second and the third steps in the above procedure, which gives no explanation of which mass should be used. Furthermore, when q^0 and q are the same flavors then (9) results in infinity which violates the analytic property of the amplitude. Even without the singularity, the factor $m_B = (m_q - m_{q^0})$ in (9) enhances the amplitude of Q_6 greatly, which is difficult to understand.

4

Now we turn to the PQCD calculations of the penguin amplitudes. In this method, no explicit use of the factorization hypothesis is needed. We cannot resolve the ambiguity of the quark masses described above. However, this ambiguity is less serious than that in the BSW model.

Following [9], we take the interpolating fields for the mesons as

$$\begin{aligned} B &= \frac{1}{\sqrt{2}} \frac{I_c}{\sqrt{3}} \bar{\psi}_B(x) \gamma_5 (\psi - m_B); \\ Y &= \frac{1}{\sqrt{2}} \frac{I_c}{\sqrt{3}} \bar{\psi}_Y(y) \gamma_5 \psi_Y; \\ Z &= \frac{1}{\sqrt{2}} \frac{I_c}{\sqrt{3}} \bar{\psi}_Z(z) \gamma_5 \psi_Z; \end{aligned} \quad (10)$$

Here I_c is an identity in the color space, and we have neglected the masses of the final states.

The decay amplitudes can be calculated using Figure 2 and 3 for the time-like and the space-like penguins, respectively. We neglect terms proportional to the final state masses, and keep in each diagram the leading term in the expansion in x_1 , the momentum fraction carried by the light anti-quark in the B meson. Denoting

$$\langle Y Z | \mathcal{O}_i | B \rangle = A_{ia} + A_{ib} + \dots + \frac{1}{i!} A_{if} \quad (11)$$

where A_{ik} ($k = a, b, \dots, f$) is the contribution from the k -th diagram of Figure 2 or 3. When the diagrams have the topology which can induce the processes, the results are summarized in the following.

(a) The time-like penguins:

$$\begin{aligned}
A_{3c}^{\text{time}} &= \frac{8g_s^2}{3^6} \frac{Z_1}{6^0} [dx][dy][dz]_B(x)_Y(y)_Z(z) \frac{4(2x_1 + y_1 + 1)}{x_1(x_1 - y_1)(2x_1 - y_1)}; \\
A_{3d}^{\text{time}} + A_{3e}^{\text{time}} &= \frac{8g_s^2}{3^6} \frac{Z_1}{6^0} [dx][dy][dz]_B(x)_Y(y)_Z(z) \frac{4}{x_1(x_1 - y_1)(x_1 - z_1)}; \quad (12)
\end{aligned}$$

$$\begin{aligned}
A_{3a}^{\text{time}} &= A_{3b}^{\text{time}} = A_{3f}^{\text{time}} = 0; \\
A_{4a}^{\text{time}} &= \frac{8g_s^2}{3^6} \frac{Z_1}{6^0} [dx][dy][dz]_B(x)_Y(y)_Z(z) \frac{12(2x_1 + y_1 + 1)}{x_1(x_1 - y_1)(2x_1 - y_1)}; \\
A_{4b}^{\text{time}} &= A_{4c}^{\text{time}} = A_{4d}^{\text{time}} = A_{4e}^{\text{time}} = A_{4f}^{\text{time}} = 0; \quad (13)
\end{aligned}$$

$$A_{5a}^{\text{time}} = A_{5b}^{\text{time}} = A_{5c}^{\text{time}} = A_{5d}^{\text{time}} + A_{5e}^{\text{time}} = A_{5f}^{\text{time}} = 0; \quad (14)$$

$$A_{6a}^{\text{time}} = A_{6b}^{\text{time}} = A_{6c}^{\text{time}} = A_{6d}^{\text{time}} = A_{6e}^{\text{time}} = A_{6f}^{\text{time}} = 0; \quad (15)$$

where $[dx] = dx_1 dx_2$, $[dy] = dy_1 dy_2$, $[dz] = dz_1 dz_2$.

(b) The space-like penguins:

$$\begin{aligned}
A_{3a}^{\text{space}} &= A_{3b}^{\text{space}} = A_{3e}^{\text{space}} + A_{3f}^{\text{space}} = 0; \\
A_{3c}^{\text{space}} &= \frac{8g_s^2}{3^6} \frac{Z_1}{6^0} [dx][dy][dz]_B(x)_Y(y)_Z(z) \frac{4}{(1 - y_1)(x_1 - x_1 y_1 + x_1 z_1 - y_1 z_1 + y_1 - 1)}; \\
A_{3d}^{\text{space}} &= \frac{8g_s^2}{3^6} \frac{Z_1}{6^0} [dx][dy][dz]_B(x)_Y(y)_Z(z) \frac{4}{z_1(1 - y_1)(x_1 - z_1)}; \quad (16)
\end{aligned}$$

$$\begin{aligned}
A_{4a}^{\text{space}} &= \frac{8g_s^2}{3^6} \frac{Z_1}{6^0} [dx][dy][dz]_B(x)_Y(y)_Z(z) \frac{12}{z_1(1 - y_1)}; \\
A_{4b}^{\text{space}} &= \frac{8g_s^2}{3^6} \frac{Z_1}{6^0} [dx][dy][dz]_B(x)_Y(y)_Z(z) \frac{12}{z_1(1 - y_1)}; \quad (17) \\
A_{4k}^{\text{space}} &= 0 \quad (k = c; d; e; f);
\end{aligned}$$

$$A_{5k}^{\text{space}} = 0 \quad (k = a; b; \quad f); \quad (18)$$

$$A_{6k}^{\text{space}} = 0 \quad (k = a; b; \quad f); \quad (19)$$

In (12-19) $g_s = \frac{g}{4}$ is the coupling constant of QCD.

Independent of the special choices of the wavefunctions, we can draw some general conclusions in the PQCD method. First, from (19), the space-like penguin contribution from the operator Q_6 vanishes, and thus the singularity due to the degeneration of the quark masses disappears. This is in sharp contrast to the observation within the BSW model discussed above.

Second, comparing the right-hand-sides of equations (16-19) and those of equations (12-15), it is obvious that the contributions from the space-like penguins are always suppressed compared to those from the time-like penguins by a factor of x_1 , the momentum fraction carried by the light quark inside the B meson, which is taken to be $0.05 \ll x_1 \ll 0.1$ [8, 9] in the PQCD method. This suppression of the space-like penguins reflects the mechanism of the helicity-suppression, as stated in [6].

5

To get the quantitative estimates, we take the wave functions as [8, 9]

$$\phi_B(x) = \frac{f_B}{2} x_1^2 (1-x_1); \quad (20)$$

$$\phi_Y(y) = \frac{f_Y}{3} y_1 (1-y_1); \quad (21)$$

$$\phi_Z(z) = \frac{f_Z}{3} z_1 (1-z_1); \quad (22)$$

Performing the integrations over $[dx]$, $[dy]$ and $[dz]$, we get the final amplitudes:

$$\begin{aligned} A_{3c}^{\text{time}} &= \left(\frac{1}{2} \left[2 \ln \frac{1-x_B}{2-x_B} + \ln \frac{1-x_B}{x_B} \right] - i \right) \frac{1}{B}; \\ A_{3d}^{\text{time}} + A_{3e}^{\text{time}} &= \frac{3}{2} \frac{1}{B}; \end{aligned} \quad (23)$$

$$A_{4a}^{\text{time}} = 3 \left(\frac{1}{2} \left[2 \ln \frac{1-x_B}{2-x_B} + \ln \frac{1-x_B}{x_B} \right] - i \right) \frac{1}{B}; \quad (24)$$

$$A_{3c}^{\text{space}} = 0.936; \quad (25)$$

$$A_{3d}^{\text{space}} = 3 \left(1 - \ln \frac{1-x_B}{x_B} - i \right);$$

	BR ($B \rightarrow K^0$) (10^{-7})		BR ($B \rightarrow K K^0$) (10^{-8})	
B	without space-like penguin	with space-like penguin	without space-like penguin	with space-like penguin
0.05	8.38	8.00	10.3	9.85
0.06	5.67	5.36	6.99	6.61
0.07	4.10	3.85	5.05	4.74
0.08	3.11	2.90	3.83	3.57
0.09	2.45	2.27	3.02	2.79
0.10	1.99	1.83	2.45	2.25

Table 1: Branching ratios for $B \rightarrow K^0$ and $B \rightarrow K K^0$ with space-like penguins included or not.

when the diagram contributes to the specified decay process. The contributions of all the other diagrams vanish. Here $\mathcal{P} = \frac{4}{9} \bar{g}_s^2 f_B f_Y f_Z$.

The branching ratios for $B \rightarrow K K^0$ and $B \rightarrow K^0$, are displayed in table 1. In the numerical calculations, we have used $\tau_B = 1.62 \times 10^{-12}$ s, $f_B = 0.132$ GeV, $f_K = 0.113$ GeV, $f_\pi = 0.093$ GeV, $|V_{ts} V_{tb}| = 0.044$ and $|V_{td} V_{tb}| = 0.013$.

From Table 1, it can be found that the space-like penguins contribute only several percents to the branching ratios and are thus less important. This result is consistent with the analysis we have carried out in the previous section.

6

We have carried out the analysis on the effects of the space-like penguin diagrams within the PQCD method. General suppressions of the space-like penguins are found compared to the time-like penguins. Numerically, the space-like penguins contribute only several percents in the penguin dominated processes $B \rightarrow K^0$ and $B \rightarrow K K^0$. We conclude that

space-like penguins are less important in this method.

We thank G. Eilam, M. Gronau, G. Kramer, P. Singer, D. Wyler, and Z.-Z. Xing for helpful discussions. The research of D.-X. Z. was supported in part by Grant 5421-3-96 from the Ministry of Science and the Arts of Israel.

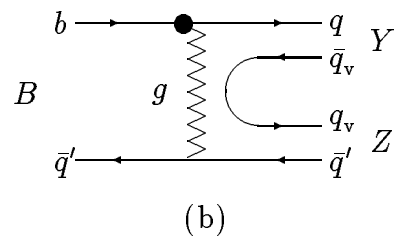
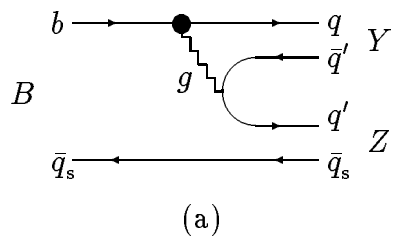
References

- [1] M. Bander, D. Silverman, and A. Soni, Phys. Rev. Lett. 43 (1979) 242; M. B. Gavela et al., Phys. Lett. B 154 (1985) 425; L. L. Chau and H. Y. Cheng, Phys. Rev. Lett. 59 (1987) 958; J. M. Gerard and W. S. Hou, Phys. Lett. B 253 (1991) 478, Rev. D 43 (1991) 2909; M. Gronau, J. L. Rosner, and D. London, Phys. Rev. Lett. 73 (1994) 21; A. J. Buras and R. Fleischer, Phys. Lett. B 341 (1995) 379; G. Kramer, W. F. Palmer and H. Simma, Z. Phys. C 66 (1995) 429; G. Kramer and W. F. Palmer, Phys. Rev. D 52 (1995) 6411.
For a review, see: G. Buchalla, A. J. Buras and M. E. Lautenbacher, preprint MPI-
PH/95-104, to be published in Rev. Mod. Phys. (1996).
- [2] D. Du and Z.-Z. Xing, Phys. Lett. B 349 (1995) 275.
- [3] D. Du, M.-Z. Yang and D.-Z. Zhang, Phys. Rev. D 53, 249 (1996).
- [4] M. Baur, B. Stech and M. Wirbel, Z. Phys. C 34, 103 (1987).
- [5] H.-Y. Cheng and B. Tseng, Phys. Rev. D 51 (1995) 1199; M. Gourdin, A. M. Kamal, Y. Y. Keum and X. Y. Pham, Phys. Lett. B 333 (1994) 507; A. N. Kamal, A. B. Santra, F. Ghoddoussi, preprint Alberta Thy 01-96.

- [6] L. L. Chau, H. Y. Cheng, W. K. Sze, H. Yao, and B. Tseng, Phys. Rev. D 43 (1991) 2176; J. Bernabeu and C. Jarlskog, Z. Phys. C 8 (1981) 233.
- [7] G. Buchalla et al, Reference [1].
- [8] A. Szczepaniak, E. M. Henley and S. J. Brodsky, Phys. Lett. B 243, 287 (1990); C. E. Carlson and J. Milana, Phys. Rev. D 49, 5908 (1994); Phys. Lett. B 301, 237 (1993).
- [9] H. Simma and D. Wyler, Phys. Lett. B 272, 395 (1991).

Figure captions

1. Time-like (a) and space-like (b) penguin diagrams.
2. Graphs for the time-like penguins in PQCD. Here the dashed-lines denote the gluons, and the crosses denote the possible quark-gluon vertices.
3. Graphs for the space-like penguins in PQCD.



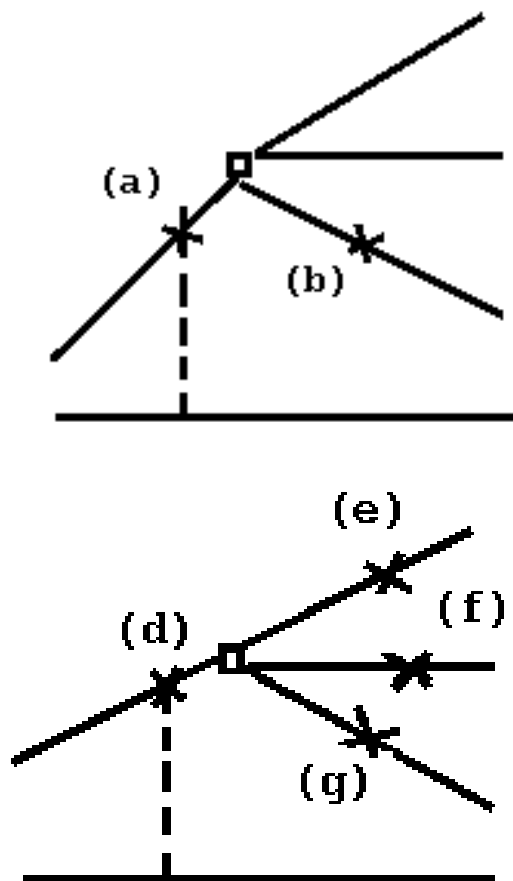


Figure 2:

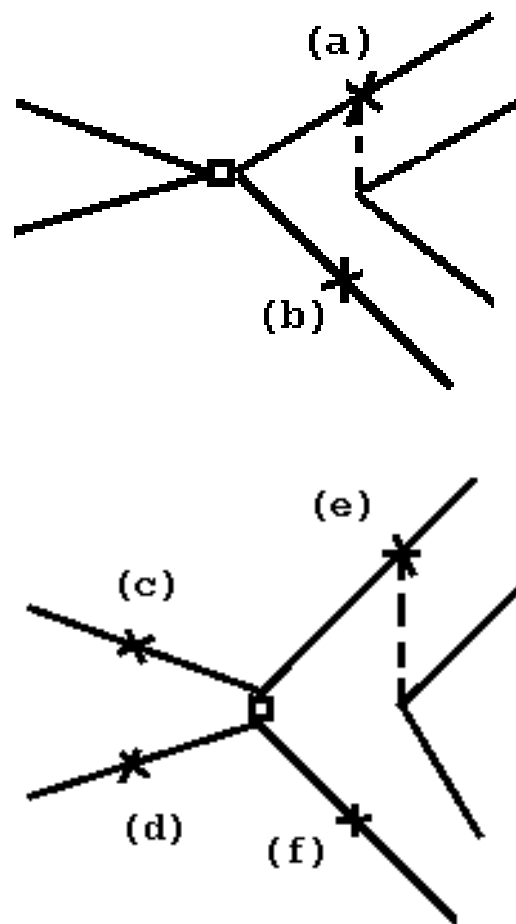


Figure 3: